Journal of Cleaner Production 370 (2022) 133545

Contents lists available at ScienceDirect

Journal of Cleaner Production

journal homepage: www.elsevier.com/locate/jclepro

Recycling waste glass aggregate in concrete: Mitigation of alkali-silica reaction (ASR) by carbonation curing

Zhuo Liu [a], Caijun Shi [b], Qiantao Shi [a], Xiao Tan [a], Weina Meng [a,*]

[a] Department of Civil, Environmental and Ocean Engineering, Stevens Institute of Technology, 614 River Terrace, Hoboken, NJ, 07030, United States
[b] College of Civil Engineering, Hunan University, 2 South Yueshan Road, Changsha, Hunan Province, 410012, China

ARTICLE INFO

Handling Editor: Prof. Jiri Jaromir Klemeš

Keywords:
Alkali-silica reaction (ASR)
Carbonation curing
Glass mortar (GM)
Microstructure
Pore solution
Recycled glass

ABSTRACT

Concerns on low rate of glass recycling are rising due to the environmental issues caused by landfills of waste glass. Glass utilization in concrete is a promising approach to vastly improve the glass recycling rate. However, the glass in concrete causes deleterious alkali-silica reaction (ASR), which cracks the concrete and weakens its durability and is the biggest challenge for this approach. To address this challenge, this study proposes the use of carbonation curing to mitigate ASR of mortar prepared with recycled glass (named glass mortar, GM) for the first time. The effects of glass content and carbonation curing regime on mechanical properties and the resistance to ASR-induced volume change of GM were experimentally investigated. It was found that although the increase of glass content had negative impact on compressive strength and resistance to ASR of GM, with optimized carbonation curing, the 28-day compressive strength was improved by up to 40%, and the ASR-induced expansions was significantly reduced by up to 85%. In addition, the underlying mechanisms of ASR mitigation by carbonation curing were further elucidated through characterization tests including thermogravimetric analysis, pore structure analysis, and pore solution analysis. The test results demonstrated that carbonation curing mitigated the ASR in GM by reducing calcium hydroxide content and the volume of pore solution, densifying the microstructure, and reducing the pH and free alkali metal content in the pore solution. This research is hopeful to promote the application of recycling glass in the concrete industry.

1. Introduction

More than ten million tons of waste glass are produced in the United States every year, and the recycling rate is concerning. About 60% of the waste glass is landfilled, while less than 20% is recycled (U. EPA, 2020), as depicted in Fig. 1. It is estimated that the amount of landfilled waste glass will be largely increased; however, the space available for landfills is shrinking. Waste glass is non-biodegradable and can permanently fill up valuable space (Jani and Hogland, 2014). In addition, the landfill of waste glass pollutes the soil and underground water because some types of glass contain hazardous materials, such as dioxins and heavy metals (Guo et al., 2020). Therefore, it is increasingly attractable to develop suitable approaches for recycling waste glass.

Although the waste glass can be recycled for new glass products, the recycling rate is still low, because the waste glass can be contaminated, color-mixed, or even broken in the processes of the waste collection, which fails for high-quality products (Kou and Poon, 2009). Therefore, it is of keen interest to develop alternative approaches to increase the recycling rate of the waste glass. One example is to re-utilize the waste glass as concrete raw materials. With 70% SiO_2 by mass, the waste glass can be crushed and sorted into desired particle sizes as aggregates or as a pozzolanic material for concrete to provide comparable or even improved performance (Topcu and Canbaz, 2004; Shao et al., 2000; Corinaldesi et al., 2005; Park et al., 2004; Johnston, 1974; Aliabdo et al., 2016; Song et al., 2019). Many benefits have been identified from using recycled glass in concrete. These include the ability to (1) increase the flowability of concrete due to the smooth surface and high density of glass (Bueno et al., 2020), (2) to reduce the cost, carbon footprint, and embodied energy of the concrete (Bostanci et al., 2018; Zhan et al., 2013), (3) and to enhance mechanical properties when glass is used as cementitious materials or as properly tailored fine aggregates (Taha and Nounu, 2008; Ling and Poon, 2011). However, in order to utilize recycled glass in concrete at a large scale, the biggest challenge that must be addressed is the alkali-silica reaction (ASR) induced by the glass (Saccani and Bignozzi, 2010; Yang et al., 2019).

ASR refers to a deleterious swelling reaction that occurs over time in

* Corresponding author.
E-mail address: weina.meng@stevens.edu (W. Meng).

https://doi.org/10.1016/j.jclepro.2022.133545
Received 9 February 2022; Received in revised form 15 July 2022; Accepted 5 August 2022
Available online 11 August 2022
0959-6526/© 2022 Elsevier Ltd. All rights reserved.

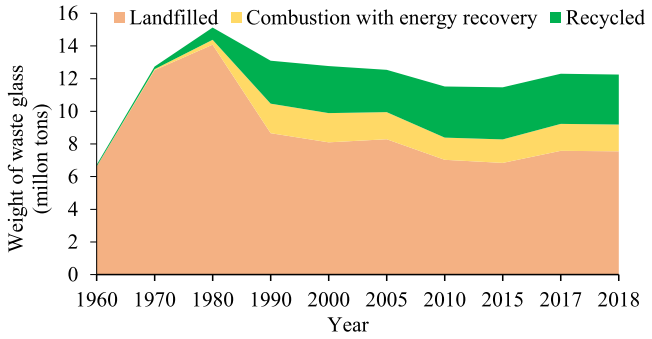

Fig. 1. The total number of tons of waste glass generated, recycled, combusted with energy recovery, and landfilled in the United States from 1960 to 2018 (U. EPA, 2020).

cementitious materials between the highly alkaline cement paste and the reactive silica in aggregates. The reaction generates ASR gel that can absorb moisture and cause expansion, subsequentially introducing internal tensile stresses and leading to concrete degradation (Thomas, 2011; Sanchez et al., 2017). Four key factors have been observed attributed to the ASR: reactive silica, alkali metals, moisture, and sufficient pH; and ASR will not occur if one of the key factors is absent. Besides, ASR can also be effectively mitigated if the content of any of the four components is reduced (Ichikawa and Miura, 2007). When glass is used as supplementary cementitious materials (SCM), the high alkali metal content in the glass can react with reactive silica in aggregates and subsequently cause deleterious ASR expansion (Serpa et al., 2013; Zheng, 2016). When the glass is used as an aggregate, it can greatly aggravate the ASR also, because glass aggregates containing reactive silica generates expansive ASR gel which degrades concrete after several years (Tapas et al., 2021; Shafaatian et al., 2013). Therefore, numerous studies has been conducted to mitigate the ASR of concrete with recycled glass as aggregates. The existing methods to suppress ASR could be summarized by the following:

(1) The use of SCMs to replace cement can reduce ASR from a material perspective. The incorporation of SCMs leads to a reduction of the concentration of alkali-hydroxides in the pore solution by binding alkali metals, thus limiting the availability of alkali metals for ASR (Thomas, 2011; Tapas et al., 2021; Shafaatian et al., 2013).
(2) The use of lithium compounds can stop the ASR from a chemical perspective. Amorphous or crystalline products containing silicon and lithium may form on the surface of reactive silica (i.e., glass aggregate), acting as a protective barrier against alkali metal ions (Aiqin et al., 1999; Du and Tan, 2013). Although the capability of mitigating ASR of concrete with glass aggregate using these methods has proven to exist, the mitigation effect is insignificant (Aiqin et al., 1999; Du and Tan, 2013; Feng et al., 2005, 2010; Kawamura and Fuwa, 2003; Ekolu et al., 2007). For example, 50% replacement of cement with fly ash reduced the ASR expansion of mortar bar with recycled glass with fine aggregates from 0.4% to 0.2%. However, the expansion is still much higher than the safe limit of 0.1% in standard ASR tests. To conclude, the effectiveness of lithium compounds on ASR mitigation of GM significantly changes with the types of lithium compounds (e.g., LiCl, $LiNO_3$, Li_2CO_3, etc.) and glasses (e.g., clear glass, brown glass, green glass, etc.) utilized (Du and Tan, 2013; Feng et al., 2005, 2010; Kawamura and Fuwa, 2003; Ekolu et al., 2007).

Therefore, more effective methods need to be explored to mitigate ASR in cementitious materials with glass. One promising approach is carbonation curing. Carbonation curing is a curing method that exposes cementitious materials to a CO_2-rich environmental chamber at an early age to form carbonation products. Meanwhile, CO_2 can also be permanently sequestered in cementitious composites to reduce the carbon footprint. Carbonation curing has previously been demonstrated to improve the compressive strength over 28 days by 40%–100% bydensifying the microstructure by filling the nano-size pores with $CaCO_3$ particles which enhancing the durability of cementitious materials (Ashraf, 2016; Šavija and Luković, 2016; Chen and Gao, 2019; Pan et al., 2017; Ashraf et al., 2019). Considering the changes of chemical and physical properties of cementitious composites caused by carbonation curing (Belda Revert et al., 2018; Mo et al., 2016; Zhan et al., 2019; Jang and Lee, 2016; Rostami et al., 2012), it is hypothesized that carbonation curing can reduce the pH, moisture content, and alkali metal content-three key components attributed to ASR. The hypothesis can be categorized in three aspects: (1) Carbonation curing could reduce the pH to a certain degree because the calcium hydroxide can react with CO_2 and partially transform into calcium carbonate. The pH plays a vital role in ASR because essentially ASR occurs when reactive silica is attacked in a high concentration of hydroxide (OH^-) ions. The maximum pH to prevent a deleterious ASR for reactive aggregate is suggested to be 13.2–13.4 (Thomas, 2011); (2) Carbonation curing could reduce the moisture content to a certain degree by facilitating the formation of nano-$CaCO_3$ to fill the pores of the concrete surface and to prevent water from penetration; (3) Carbonation curing could affect the free alkali metal content in the pore solution to a certain degree because the alkali metal binding capacity is linked with the structure of C–S–H, which can be essentially changed by carbonation (L'Hôpital et al., 2016a; De Weerdt et al., 2019a). Overall, the combined effects of carbonation curing are assumed to be able to significantly mitigate ASR.

To validate the hypothesis, the overarching goal of this study is to investigate the effects of carbonation curing on mitigating ASR in concrete with recycled glass. Specifically, this paper has three main objectives: (1) to propose an experimental approach of carbonation curing for mitigating ASR of mortar prepared with recycled glass fine aggregates (or named as glass mortar, GM); (2) to investigate the effects of glass content and carbonation curing duration on mechanical properties and the ASR resistance of GM; (3) to understand and further interpretate the underlying mechanisms of improving ASR resistance by carbonation curing through characterization tests, including thermogravimetric analysis, pore structure analysis, and pore solution analysis. Compared with previous research on mitigation of ASR of cementitious materials with recycled glass, this research is novel in three aspects: (1) This study utilizes carbonation curing to mitigate ASR of cementitious materials prepared with recycled glass fine aggregates for the first time. (2) This study develops an optimized carbonation curing condition, which can significantly improve the compressive strength and the ASR resistance of cementitious materials with recycled glass. (3) The underlying mechanisms of carbonation curing are promising in efficiently mitigating ASR in cementitious materials with recycled glass and advancing the application of recycling glass in concrete. To the end, GMs were prepared using 20% and 40% recycled glass to replace river sand. The effects of carbonation durations and glass content on the mechanical properties and ASR-induced volume change of the GM were investigated. To understand the underlying mechanisms, experiments on GM mixtures with/without carbonation curing were conducted to characterize and compare their phase evolutions by thermal thermogravimetric analysis (TGA), porosity developments by mercury intrusion porosimetry (MIP), changes of pH, and free alkali metal content in the pore solution by cold water extraction (CWE) method.

2. Materials and mixture design

2.1. Raw materials

This research adopted Type I Portland cement, river sand, recycled

glass, chemical admixtures, and tap water. The chemical compositions of the Type I Portland cement, river sand, and recycled glass were characterized by X-ray fluorescence (XRF) and X-ray diffraction (XRD), as listed in Table 1. A polycarboxylate-based high-range water reducer (HRWR) is used to improve the flowability. The water reducing rate of the HRWR is 30%, and the solid content and specific gravity of the HRWR are 34.4% and 1.05, respectively. The particle size distribution of the cement was characterized using a laser diffraction particle size analyzer. Particle size distributions of the river sand and recycled glass were characterized using ASTM sieves (ASTM C136, 2015) and presented in Fig. 2. Their particle size distribution curves show that river sand is finer than recycled glass, with the mean size of river sand approximately half of that of recycled glass.

2.2. Mixture design

The mixture design of investigated mixtures is shown in Table 2. All mixtures have a fixed water-to-cement ratio of 0.5 and a sand-to-binder ratio of 2.25. To investigate the effect of recycled glass on ASR, two groups of mixtures were prepared: GM mixtures with 20% and 40% river sand replaced by recycled glass by volume. To investigate the effect of carbonation curing on mitigating ASR, each group of mixtures was carbonation-cured for 0 h, 6 h, and 12 h at early ages. In Table 2, the identifications of all mix designations are labelled according to the test parameters. For example, the designation "RG20C6" indicates that the mixture is prepared using 20% recycled glass to replace river sand and carbonation curing duration of 6 h.

2.3. Mixing and curing

A 5-L mixer (model: Horbart) was used to mix materials in this study, and the mixing processes can be divided in four steps: (1) Mix all dry ingredients (cement, river sand, and recycled glass) at 60 rpm for 90 s; (2) dissolve HRWR in 80% of the required tap water by stirring the HRWR-added water with a glass rod, then add it to the mixer and mix at 120 rpm for 2 min; (3) add the rest of water and mix at 120 rpm for 1 min; (4) stop the mixer and scrape it and mix for another 1 min at 120 rpm. After mixing, GM prism samples were casted in 25 mm × 25 mm × 250 mm molds to measure length changes for ASR expansion test, and GM cubic samples were casted in 50 mm × 50 mm × 50 mm molds to measure compressive strengths. The casted samples were then covered with plastic sheets immediately after consolidation and cured at a temperature of 20 ± 3 °C and a relative humidity of 60% ± 10% for 20 h, then the specimens were demolded for further curing.

The steps of the curing process for samples are shown in Fig. 3. After the 20 h of in-mold curing, all samples were demolded for further curing.

Table 1
Chemical and physical properties of raw materials.

Content	Type I cement	River Sand	Recycled glass
SiO_2 (%)	22.44	86.50	76.01
Al_2O_3 (%)	2.76	0.39	3.37
Fe_2O_3 (%)	2.24	1.47	0.02
CaO (%)	68.05	9.42	5.80
MgO (%)	0.91	–	0.91
SO_3 (%)	2.25	–	0.65
Na_2O (%)	0.19	–	11.30
K_2O (%)	0.04	–	0.72
TiO_2 (%)	0.14	–	0.05
P_2O_5 (%)	0.09	–	0.02
Mn_2O_3 (%)	0.03	–	0.01
SrO (%)	–	–	–
C_3S (%)	62.35	–	–
C_2S (%)	20.28	–	–
C_3A (%)	1.42	–	–
C_4AF (%)	5.83	–	–
LOI (%)	1.28	0.24	0.4%
Specific gravity	3.15	2.64	2.56

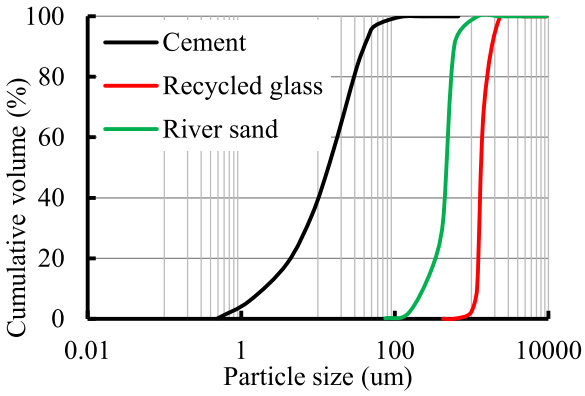

Fig. 2. Particle size distribution of cement, river sand, and recycled glass.

Table 2
Mix designations and proportions of GM mixtures (kg/m^3).

Designation	Cement	Water	River sand	Recycled glass	HRWR	CO_2 curing
RG20C0	590.9	295.5	1063.7	260.0	3.0	0 h
RG20C6	590.9	295.5	1063.7	260.0	3.0	6 h
RG20C12	590.9	295.5	1063.7	260.0	3.0	12 h
RG40C0	590.9	295.5	797.8	520.0	3.0	0 h
RG40C6	590.9	295.5	797.8	520.0	3.0	6 h
RG40C12	590.9	295.5	797.8	520.0	3.0	12 h

First, all samples were dried in an environmental chamber at a temperature of 30 °C and a relative humidity of 30% for 4-h pre-curing. The purpose of the pre-curing was to decrease the number of water-filled pores to allow faster diffusion of CO_2 gas into the GM samples (Shi et al., 2012; Zhang et al., 2018). After that, GM samples of each mixture was divided into three groups for carbonation curing, each group includes 2 mixtures and each mixture includes 9 cubics for compressive tests and 3 prisms for ASR tests: (1) Samples of Group 1 (RG20C0 or RG40C0) were sealed in a plastic bag and put in the environmental chamber at a temperature of 30 °C and a relative humidity of 60% for 12h; (2) Samples of Group 2 (RG20C6 or RG40C6) were put in the carbonation chamber for 6 h and then sealed for 6 h; and (3) Samples of Group 3 (RG20C12 or RG40C12) were put in carbonation chamber for 12 h. The carbonation chamber was vacuumed first and then supplied with CO_2 gas (purity: 99.9%) until the partial pressure increased to 0.3 MPa. The chamber was kept at a temperature of 30 °C and a relative humidity of 60%. After carbonation curing, the GM prism samples were utilized for ASR expansion tests, and GM cubic samples were further moisture-cured in a water tank at a temperature of 30 °C and a relative humidity of 60% until testing ages for measuring compressive strength at 1d, 7d, 28d.

3. Experiment program

3.1. Compressive strength and ASR test

3.1.1. Compressive strength

The compressive strength at 36 h (referring to compressive strength at 1 day), 7 days, and 28 days were evaluated using 50 mm × 50 mm × 50 mm cubic samples, according to ASTM C109 (ASTM C109, 2020). The loading rate for the testing was kept at 1.8 kN/min.

3.1.2. ASR expansion

ASR expansion tests were conducted by ASTM C1567 (ASTM C1567, 2013) using 25 mm × 25 mm × 250 mm mortar bar samples, which is an accelerated test designed for mortar mixture (Shafaatian et al., 2013). After carbonation curing, the prism samples were placed in a container

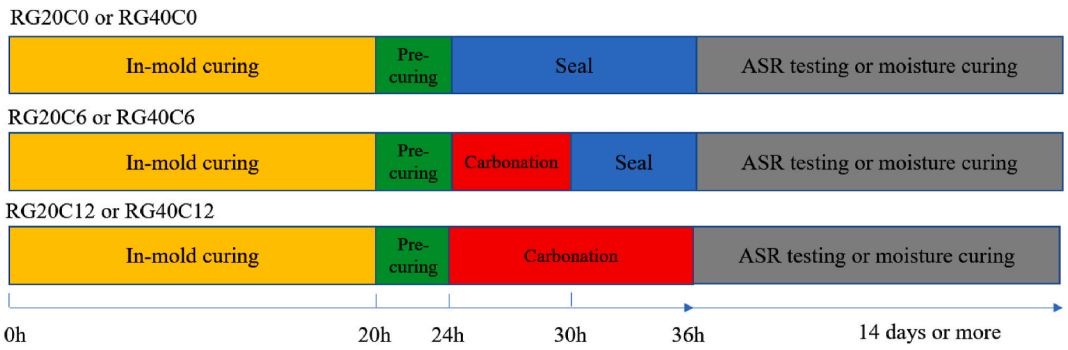

Fig. 3. Curing procedures for investigated specimens.

with sufficient tap water (at 23 °C) to immerse them. Then the container was sealed and placed in an oven at 80 °C for 24 h. After that, the container was removed from the oven. The prism samples were removed from the water and dried with a towel, and the zero reading of each prism sample was then taken immediately after drying. After recording the initial readings for all mixtures, all prism samples were placed in a container with sufficient 80 °C 1M NaOH solution. Then the container was sealed and re-placed to the oven at 80 °C. Subsequent readings of the prism samples were taken every 24 h till the 14th day after the zero reading. For each mixture, three prism samples were tested, and the expansion was determined by the average value.

3.2. Characterization tests

Characterization tests were conducted to understand and interpretate the underlying mechanisms of affecting ASR resistance by carbonation curing. Thermogravimetric analysis was conducted to explore the phase evolution during carbonation curing, pore structure analysis was conducted to study the microstructure development, pore solution analysis was conducted to investigate the changes of pH and alkali metal content in pore solution. The results of the three tests will be utilized to bridge the relationship between carbonation curing and improvement of ASR resistance.

Because carbonation is a diffusion-based process, the carbonation degree at different depths of a sample is different (i.e., the front-end has a higher carbonation degree than that of the midsection). Therefore, the front-end and the midsection of the carbonated sample need to be analyzed separately for characterization tests, including three samples for the thermogravimetric analysis, three samples for pore structure analysis, and three samples for pore solution analysis.

To prepare the samples for all characterization tests, the cubic sample was cut into three layers first using a concrete saw. Then the middle layer was cut into three prisms, and the middle prism was cut into four small pieces. Fig. 4 illustrated the location of samples for characterization tests in a GM cubic sample, where two pieces highlighted in red and green represent the front-end and the midsection respectively. These red and green pieces were then soaked in isopropanol to stop hydration and would further be used for tests introduced in the following sections.

3.2.1. Thermogravimetric analysis

Carbonation curing could generate various carbonation products, which could affect the composition of cementitious materials and the microstructure of the carbonated sample, subsequently influencing the ASR. Therefore, the phase evolution of the investigated samples was evaluated using a thermogravimetric analyzer (TGA, model: TA® TG55). About 50 mg of powder was ground from the front-end using a grinder rod and vacuum dried at room temperature for 24 h before the TGA test. During the TGA test, the sample was heated in a nitrogen flow at the flow rate of 50 ml/min, and the temperature was controlled from

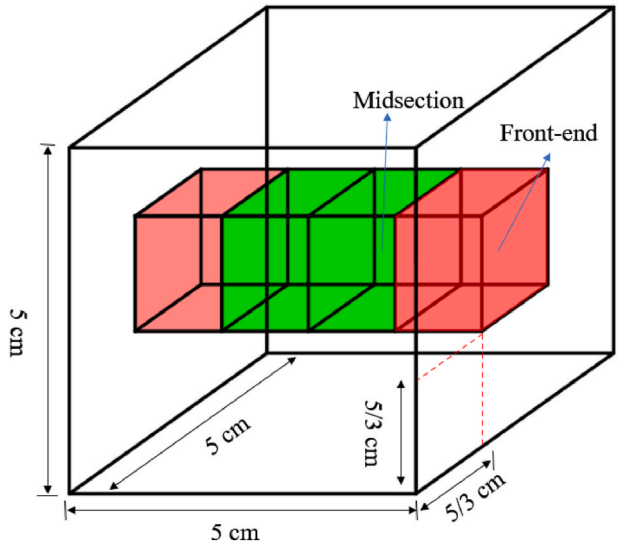

Fig. 4. Location of samples for characterization tests in a GM cubic sample.

20 °C to 1000 °C with a constant rate of 20 °C/min.

3.2.2. Pore structure analysis

Carbonation curing could lead to changes of microstructure (especially in the front-end), which could affect the permeability of the GM and thus the performance of ASR resistance. As an indicator of transport properties, the pore structures of investigated mixtures were evaluated using mercury intrusion porosimetry (MIP, model: Antor Paar Poremaster) with applied pressures ranging from 0.1 MPa to 400 MPa. The front-end pieces were used for the measurement of the porosity and pore size distribution. For each investigated mixture, approximately 1 g of sample was cut from the front-end pieces using a concrete saw and then and vacuum dried at room temperature for 24 h before testing.

3.2.3. Pore solution analysis

Weathering carbonation at late ages was reported to affect the pH and alkali metal content of the pore solution (L'Hôpital et al., 2016a; De Weerdt et al., 2019a), which are important influence factors of ASR. However, how carbonation curing at early ages affects pore solution and ASR is still unclear. Therefore, the pore solution changes including pH and alkali metal content should be investigated and the effects on ASR need to be analyzed. Cold water extraction (CWE) method was selected to determine the pH and free alkali metal content in pore solutions, which are successfully adopted by multiple studies (Alonso et al., 2012; Plusquellec et al., 2017; Räsänen and Penttala, 2004).

Procedures for pore solution analysis using the cold water extraction method is illustrated in Fig. 5. First, a suspension was prepared using 2.5

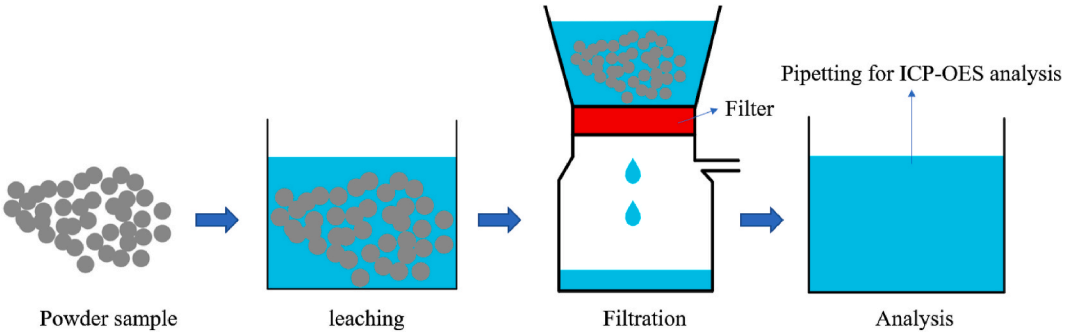

Fig. 5. Procedures for pore solution analysis using cold water extraction method (Plusquellec et al., 2017).

g of powders ground from a solid sample at age of 28d and 50 g of deionized water. They are mixed and stirred on a magnet stirrer at 800 rpm for 5 min to enable ions in pore solution to leach out. Then, the pH value of the prepared suspension was measured by a pH meter with 2-point calibration. It should be noted that the measured pH value of the suspension is not equivalent to the real pore solution pH, but it is associated with the released alkali metals from the pore solution. The measured pH value is smaller than the pore solution pH value because the extracted pore solution is diluted to the suspension with large water-to-solid ratio (20 for this study). A study showed that the pH of the suspension changed in an exponential function with the change of the pH of the pore solution, and the suspension pH could be used to assess the degree of pH change (Räsänen and Penttala, 2004). Next, the suspension was filtrated using a glass fiber filter with a pore size of 2 μm. Preliminary investigations showed that there was no significant uptake of ions by the filter and no release/adsorption of alkali metals from the sand used (Räsänen and Penttala, 2004). Finally, each solution was acidified using 40% HNO_3 to obtain a 1% HNO_3 concentration. The solutions were analyzed for Na^+ and K^+ using inductively coupled plasma - optical emission spectrometry (5100 ICP- OES, Agilent, United States).

Based on the ICP-OES results, the free alkali metal content could be calculated with Eq. (1):

$$X = [X] \times \frac{V_{water}}{m_{sample}} \quad (1)$$

where X is either the free Na^+ and K^+ content in the sample (mmol/kg); $[X]$ is the concentration of the element in the filtrate obtained after CWE (mmol/L); V_{water} is the volume of deionized water that is added during CWE (L); and m_{sample} is the mass of the sample (kg).

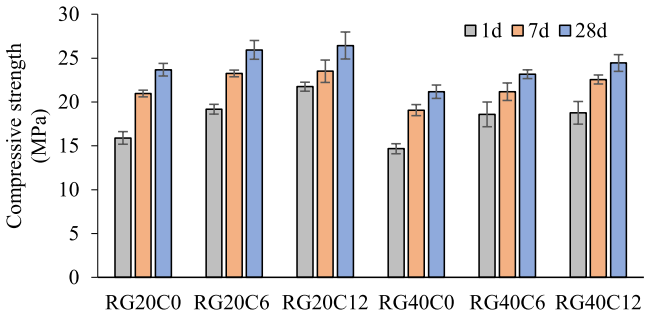

Fig. 6. Compressive strength of investigated mixtures at 1 day, 7 days, and 28 days.

4. Compressive strength and ASR expansion of GM under carbonation curing

4.1. Compressive strength

Fig. 6 presents the results of compressive strength of the investigated mixtures at 36 h (referring to compressive strength at 1 day after carbonation curing), 7 days, and 28 days.

For mixtures RG20C0 and RG40C0 without carbonation curing, as the content of recycled C0glass increased from 20% to 40%, the compressive strength at 1 day decreased from 15.9 MPa to 14.7 MPa (by 8%), and the compressive strength at 28 days decreased from 23.7 MPa to 21.2 MPa (by 11%). The reduction of compressive strength can be attributed to: (1) The use of recycled glass as fine aggregates particles weakened the interfacial bond strength because of the smooth and dense surface of glass (Kou and Poon, 2009; Taha and Nounu, 2008; Ling and Poon, 2011); (2) The homogeneousness of aggregate distribution was compromised due to the poor gradation of the waste glass (De Weerdt et al., 2019b).

For mixtures containing 20% recycled glass (RG20C0, RG20C6 and RG20C12), as the carbonation curing duration increases from 0 h to 12 h, the compressive strength at 1 day increased from 15.9 MPa to 21.8 MPa (by 37%), and the compressive strength at 28 days increased from 14.7 MPa to 18.8 MPa (by 12%). For mixtures containing 40% recycled glass (RG40C0, RG40C6 and RG40C12), as the carbonation curing duration increases from 0 h to 12 h, the compressive strength at 1 day increased from 15.9 MPa to 21.8 MPa (by 29%), and the compressive strength at 28 days increased from 21.2 MPa to 24.5 MPa (by 16%). The results indicate that carbonation curing can significantly improve the strength at both early and late ages. The compressive strength gains fast at an early age as the result of carbonation curing, which is owing to the fast carbonation reaction, precipitation of $CaCO_3$, and densified C–S–H (Liu and Meng, 2021). The carbonation reaction happens rapidly in a few hours, while the cement hydration degree is still low at early ages (Pan et al., 2019). The calcite particles generated from carbonation provide extra nucleation sites for precipitation and growth of hydration products.

It can be observed that the 28-day compressive strength of RG40C12 is 5% higher than that of RG20C0, which means that the negative impact of recycled glass on mechanical strength can be eliminated through proper carbonation curing. This result indicates the benefit of utilization of carbonation curing to mitigate the adverse effect of glass on mechanical properties of GM mixtures.

4.2. ASR expansion

The expansion results for the GM samples are shown in Fig. 7. The expansion limit of conventional concrete is 0.10%, as defined in the ASTM standard (ASTM C1567, 2013). Any mixture that has an expansion more than the limit value is stated to have potentially deleterious reactivity of aggregates.

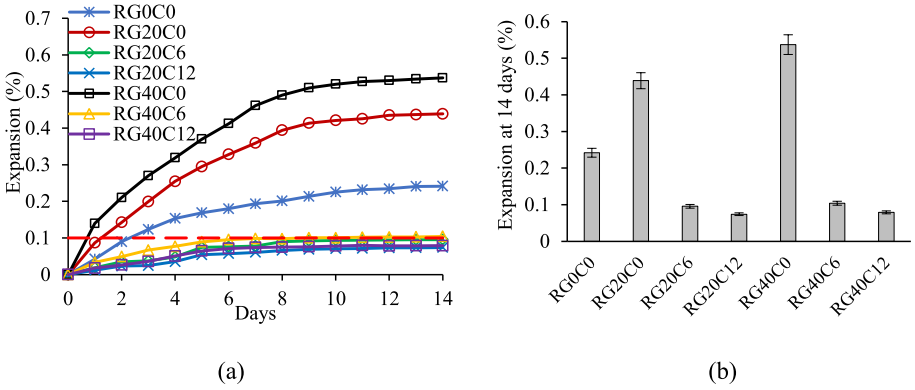

Fig. 7. ASR expansion of investigated mixture: (a) expansion as a function of time, (b) expansion at 14 days.

It is observed that the ASR-induced expansion for GM samples without exposing to carbonation curing (RG0C0, RG20C0, and RG40C0) exceeded the expansion limit within three days and reached 0.24%, 0.44%, and 0.54% in 14th day, respectively, which confirms that the ASR of mixtures without carbonation curing was significant and increase of glass content dramatically intensified the ASR.

According to Fig. 7, with the carbonation curing, the ASR was significantly mitigated. The ASR-induced expansions of all the GM samples exposed to carbonation curing were reduced below the safety limit at 14th day except that of R40C6 mixture, which is only slightly above the safety limit. For mixtures with 20% recycled glass (RG20C0, RG20C6 and RG20C12), as carbonation curing duration proceeds from 0 to 12 h, the ASR-induced expansion on Day 14 is reduced from 0.44% to 0.074% (by 86%). For mixtures with 40% recycled glass (RG40C0, RG40C6 and RG40C12), the ASR-induced expansion on Day 14 is reduced from 0.54% to 0.079% (by 85%). Because there was a high degree of ASR mitigation, this shows the significant effectiveness of the proposed method and its advantageous over other existing methods for ASR mitigation discussed in previous studies (Aiqin et al., 1999; Du and Tan, 2013; Feng et al., 2005, 2010; Kawamura and Fuwa, 2003; Ekolu et al., 2007).

The results indicate the promising effects of carbonation curing in mitigating ASR. The reduction of ASR-induced expansion in carbonated mixtures could be attributed to multiple reasons: (1) Carbonation curing could reduce the alkalinity because the calcium hydroxide can react with CO_2 and partially transform into calcium carbonate. (2) Carbonation curing could reduce the moisture content by facilitating the forming of nano $CaCO_3$ to fill the pores of mortar surface and prevent water from penetration; (3) Carbonation curing could reduce the alkali metal ions in the pore solution because of physically binding by calcium silicate. These hypotheses were further investigated and discussed in the Section 5.

5. Discussions on mechanisms of ASR mitigation by carbonation curing

This section fully discusses the underlying mechanisms of the ASR mitigation by carbonation curing. Specifically, based on the hypothesis: (1) Discussion on phase evolutions of GM mixtures was conducted through thermogravimetric analysis reactive glass, which is presented in Section 5.1. (2) Discussion on microstructure developments of GM mixtures was implemented according to pore structure analysis, which is presented in Section 5.2. (3) Discussion on changes of pH and free alkali metal content in the pore solution of GM mixtures was carried out based on the elemental analysis of pore solution, which are presented in Sections 5.3.1 and 5.3.2.

5.1. Phase evolutions

Fig. 8 illustrates the thermogravimetry analysis for mixtures RG20C0, RG20C6, and RG20C12, which were applied with different carbonation curing durations. Fig. 8(a) and (b) show weight change and differential weight change of the samples under rising temperatures, respectively. It is observed that each sample exhibited three obvious peak shapes corresponding to dehydration (105 °C–300 °C), dihydroxylation (420 °C–480 °C), and decarbonation (600 °C–950 °C). Based on the induced weight losses at the temperature range, the amount of $Ca(OH)_2$ and $CaCO_3$ can be roughly calculated. The calculated content of $Ca(OH)_2$ and $CaCO_3$ in each sample are presented in Fig. 8(c) and (d), respectively.

As the carbonation curing duration increased from 0 h to 12 h, the $Ca(OH)_2$ content was firstly reduced from 3.2% to 1.3% and then increased to 1.7%. The reason for reduction of $Ca(OH)_2$ is that the carbonation reactions transform $Ca(OH)_2$ to $CaCO_3$; besides, the promoted hydration by more presence of $CaCO_3$ nanoparticles in the RG20C12 can result in the increase of $Ca(OH)_2$ compared with that in RG20C6.

As the carbonation curing duration increased from 0 h to 12 h, the $CaCO_3$ content was increased from 3.2% to 12.9%, which is owing to the increment of carbonation degree. The phase evolution contributes to ASR mitigation because the reduction of $Ca(OH)_2$ content can lead to pH drop, which further results in the less reactive glass involved in ASR; besides, the increase of $CaCO_3$ content can densify microstructure, which reduces the contact between glass and pore solution. These will be further discussed in the following two sections.

In addition, the evaporable water corresponding to mass loss within 30 °C–105 °C of mixtures RG20C6 and RG20C12 were reduced significantly compared with that of mixture RG20C0, which indicates that the free water in the GM was greatly consumed by carbonation curing and further leading to volume reduction of pore solution. Because ASR is trigged by the pore solution containing hydroxyl and glass, with the volume reduction of pore solution and calcium hydroxide, the ASR is expected to be mitigated.

5.2. Microstructure development

Fig. 9 presents the pore structure profile, including pore size distribution and porosity of RG20C0, RG20C6, and RG20C12 mixtures.

Fig. 9(a) shows that the pore size distributions of three mixtures cover pores with diameters ranging from 3 nm to 10000 nm. It can be identified that the most noticeable change of pore volume lies between the pores with diameter sizes from 5 nm to 10 nm. The peak locates at around 6 nm, which dramatically decreased from 0.799 ml/g for RG20C0 to nearly zero for RG20C12.

Fig. 9(b) indicates the porosity is constituted of three types of pores in cementitious materials: (i) Micropores with mainly gel pores (<10 nm); (ii) mesopores or capillary pores (10 nm–5000 nm); and (iii)

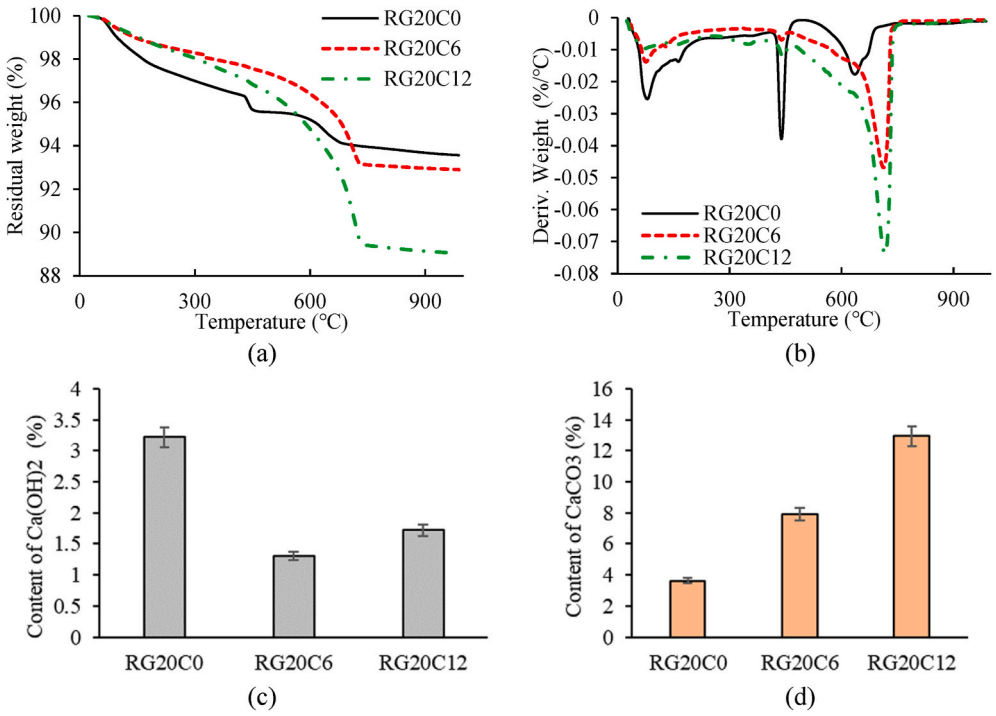

Fig. 8. TGA test results of investigated mixtures: (a) Weight changes; (b) differential weight changes; (c) content of $Ca(OH)_2$; and (d) content of $CaCO_3$.

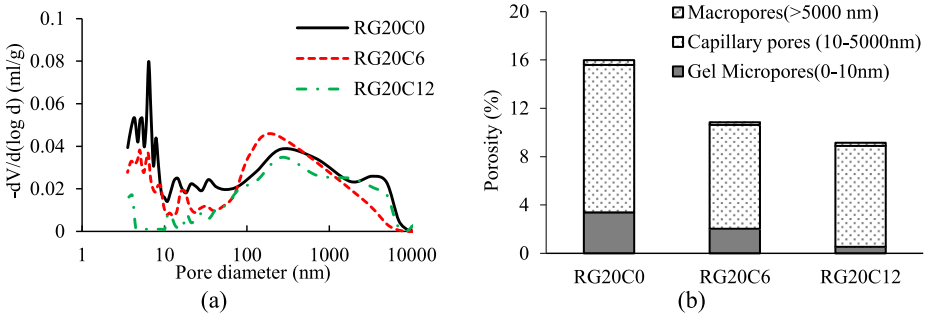

Fig. 9. Pore structure profile: (a) Pore size distribution; and (b) porosity.

macropores due to deliberately entrained air or inadequate compaction (>5000 nm) (Liu et al., 2022; Kumar and Bhattacharjee, 2003; Gong et al., 2014; Sun et al., 2019). It is concluded that the total porosity was significantly reduced in GM exposed to carbonation curing. As the carbonation duration proceeded from 0 to 12 h, the total porosity decreased from 16.0% to 9.2% (by 42%). The porosity of macropores remained relatively stable (less than 0.4%), while the reduction of micropores and capillary pores are mainly responsible for the total porosity decrease. The porosity gel micropores decreased from 3.4% to 0.5% (by 85%), and the porosity of capillary pores = reduced from 12.2% to 8.3% (by 32%).

The reason for the reduction of micropores is that CO_2 can react with the layer calcium in the C–S–H gel to form nano-$CaCO_3$ particles, which are embedded in the C–S–H gel to fill the gel pores (Liu and Meng, 2021; Zhan et al., 2021). The reduction of the capillary pore volume is mainly attributed to the precipitation of nano-sized $CaCO_3$ crystals and their nucleation effects to promote the formation of hydration products (Meng and Khayat, 2018; Zhang and Shao, 2018). The reduction of gel pores in C–S–H by carbonation can also cause some degree of shrinkage, known as carbonation shrinkage (Han et al., 2013; Borges et al., 2010), which further compensates for some expansion induced by ASR. Capillary pores are responsible for strength reduction, transport properties, and durability (Du et al., 2021). Besides, reduction of capillary pores by carbonation curing can enhance the mechanical properties of GM to resist expansive cracking and to prevent moisture and alkali metal transportation to subsequently reduce the contact among reactive silica, alkali, and moisture. Therefore, the reduction of gel pores and capillary pores by carbonation curing can benefit the ASR mitigation of GM.

5.3. *Pore solution changes*

5.3.1. *Change of pH in the pore solution*

The pH results of pore solution extracted from front-end and midsection pieces (shown in Fig. 4) of RG20C0, RG20C6, and RG20C12 are presented in Fig. 10. As the carbonation duration increased from 0 to 12 h, the pH of the extracted pore solution in the front-end was reduced from 13.4 to 12.0 (Thomas, 2011)., while the pH of that from the midsection remained almost the same. This is attributed to the CO_2 dissolved in the pore solution, and then the generated carbonic acid reacted with calcium hydroxide, which further led to a neutralization effect in the pore solution with the alkaline environment. The pH was reduced in the front-end and remained stable in the midsection, because carbonation is a process based on CO_2 diffusion from the surface to the middle, and carbonation slows down with the increase of carbonation

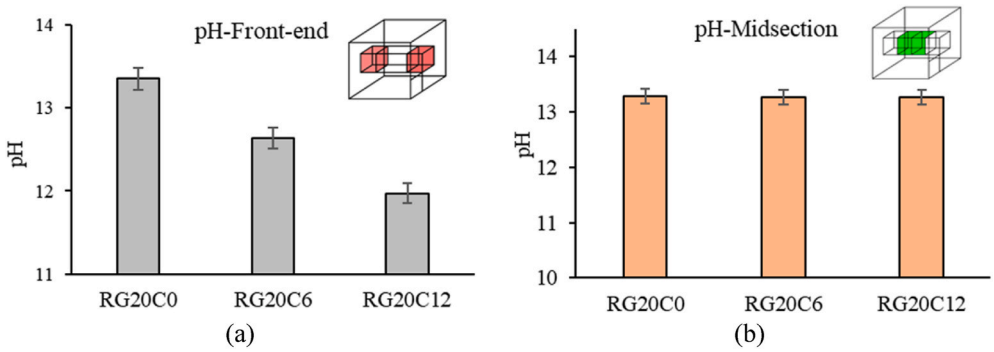

Fig. 10. The pH of the GM suspension: (a) Front-end (red); and (b) midsection (green).

depth.

As aforementioned, pH plays an important role in ASR, because reactive silica is vulnerable in high pH due to the presence of high hydroxide (OH^-) ions concentration. The maximum pH to prevent a deleterious ASR for reactive aggregate is suggested to be 13.2–13.4 (Thomas, 2011). As the pH is reduced, less reactive silica dissolves from the aggregate, which is beneficial to improve ASR resistance. It should be noted that a decrease in pH may also raise concerns on corrosion when reinforcement is used. However, the pH drop may not increase the risk of corrosion of reinforcement because (1) carbonation depth by carbonation curing is limited to the front-end, and the pH of the midsection is rarely changed. Studies demonstrated that the long-term pH of carbonation-cured concrete in depth higher than 10 mm is not reduced in long-term weathering carbonation (Zhang et al., 2020), because although a carbonation depth is formed in early-age carbonation curing, the CO_2 diffusion to internal concrete is slowed down in weathering carbonation because of the densified carbonated surface. Normally the thickness of concrete cover is more than 20 mm (Shi et al., 2004; Zhang and Shao, 2016), meaning the pH around the reinforcement is little affected. (2) densification of the surface by carbonation curing can prevent penetration of moisture and oxygen from atmosphere, which serves like an armor that protect the inside reinforcement from being attacked. Studies proved using carbonation curing as a surface treatment method is effective to enhance the gas and moisture impermeability and thus to enhance concrete durability and corrosion resistance (Pan et al., 2017, 2019). The actual impact of carbonation curing on corrosion of reinforcement will be further verified in the future study.

5.3.2. *Change of alkali metal content in the pore solution*

Fig. 11 shows the concentrations of Na^+ and K^+ in the pore solutions extracted from mixtures RG20C0, RG20C6, and RG20C12. For the mixture RG20C0 without carbonation curing, the differences of Na^+ and K^+ concentrations between the front-end and midsection were not significant, which indicates that the distribution of free alkali metals in the pore solution is homogeneous. As the carbonation curing duration

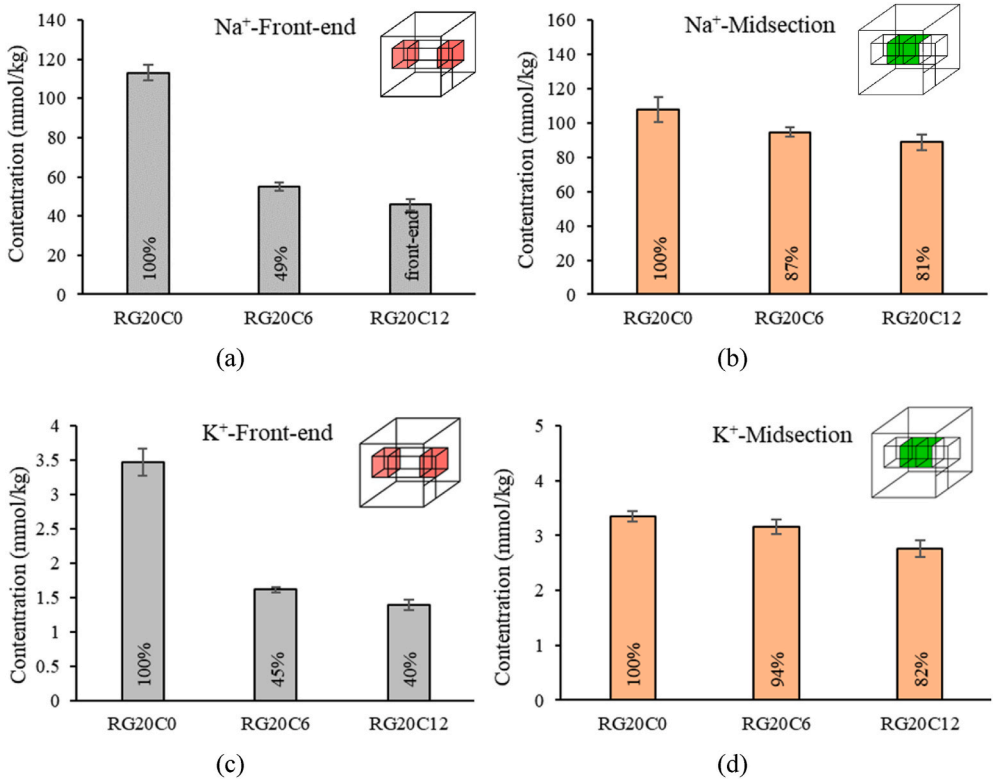

Fig. 11. Effect of carbonation curing on alkali metal content in the pore solution: (a) Na^+ in the front-end (red); (b) Na^+ in the midsection (green); (c) K^+ in the front-end (red); and (d) K^+ in the midsection (green).

increased from 0 h to 12 h, the Na^+ concentration in the front-end was reduced from 104 mmol/kg to 42 mmol/kg (by 60%), and the Na^+ concentration in the midsection was reduced from 99 mmol/L to 82 mmol/kg (by 17%). Similarly, the K^+ concentration was reduced from 3 mmol/kg to 1.3 mmol/kg (by 57%) in the front-end and from 3.1 mmol/kg to 2.5 mmol/kg (by 19%) in the midsection, respectively. The results proved that carbonation curing could lead to a reduction of alkali metal concentration in the pore solution for both the front-end and midsection of the GM, and the reduction in the front-end is more significant.

Previous studies indicated that alkali metals can be bound in the interlayer of C–S–H (L'Hôpital et al., 2016a; Hong and Glasser, 1999; Bernard et al., 2021; L'Hôpital et al., 2016b). From the above results, it is apparent that carbonation enhanced the capability of alkali metal binding due to C–S–H, which agrees with results from the C–S–H modification by carbonation (Liu and Meng, 2021; Zhan et al., 2021). The carbonation curing can lead to decalcification of C–S–H and reduction of Ca/Si in C–S–H, because (i) calcium ions are consumed by carbonation; (ii) interlayer calcium is removed; and (iii) Si–OH is condensed into Si–O–Si (Liu and Meng, 2021; Pan et al., 2019). As is shown in Fig. 12, with the reduction of interlayer Ca^{2+} ions due to precipitation of $CaCO_3$ during carbonation curing, alkali metal ions are bound into the interlayer to maintain charge balance, which caused the increase sorption of alkali metal ions and reduction of the free alkali metals in the pore solution.

Although the midsection is not carbonated according to the TGA analysis, the alkali metal content was still reduced, indicating that migration of Na^+ and K^+ occurred from the midsection to the front-end. It was found that Na^+ and K^+ in the uncarbonated area can move to the carbonated area to maintain the equilibrium concentration for the metal ions in the pore solution (Shoji et al., 2015), as shown in Fig. 13. The results further explain the reduction of alkali metals in the uncarbonated midsection area.

As discussed above, four indispensable factors for the ASR are: sufficient reactive silica, sufficient alkali metals, sufficient pH, and sufficient moisture. The carbonation curing can (i) considerably reduce the pH and amount of pore solution; (ii) effectively facilitate the binding of alkali metals and decrease transportable alkali metals; and (iii) significantly densify the microstructure and prevent the moisture and alkali metals from penetrating into the GM. Due to the combination effects, the carbonation curing can greatly mitigate the ASR of GM.

6. Conclusions and future studies

This study investigated the mortar prepared with recycled glass fine aggregates (or named as glass mortar, GM). GMs were prepared using 20% and 40% recycled glass to replace river sand, and they were exposed to 0-h ~12-h carbonation curing at early ages. The mechanical properties and ASR degradation of the GM with/without carbonation curing were investigated. Further, the underlying mechanisms, including the phase evolution, microstructure development, and changes of pore solution by carbonation curing, were deeply investigated. Based on the above investigations, the following conclusions can be drawn:

- This study introduces a technique using carbonation curing to mitigate ASR of mortar with recycled glass for the first time. For GM with 40% recycled glass and 12 h of carbonation curing, the 28-day compressive strength was increased by 18%, and ASR expansion was reduced by 86% to a value under the safe limit.
- Carbonation curing significantly reduced the content of $Ca(OH)_2$ and increased the content of $CaCO_3$, which led to a reduction of pH in the front-end from 13.4 to 12.5. As the pH is reduced, less reactive silica dissolves from the aggregate for ASR.
- Carbonation curing can densify the microstructure, reducing total porosity by 42% after 12 h ofcarbonation curing. The refinement of pore structure acts both on gel micropores and capillary pores as the result of the precipitation of nano-sized $CaCO_3$ particles and their nucleation effect that promotes the formation of hydration products.
- Carbonation curing can lead to a reduction of total pore solution volume and also free alkali metals in the pore solution (by 67% in front-end). The reduction is attributed to the fact that carbonation curing leads to decalcification of C–S–H with enhanced absorptivity of alkali metals.

Based on this research, future studies should be carried out to establish a deeper understanding of the effects of glass on the material properties of glass concrete for cleaner production and business sustainability in civil infrastructure. Below are specific opportunities to guide future research:

- To ensure the sustainability and low carbon footprint of the proposed method, future studies should conduct life-cycle analyses on cost and carbon footprint of carbonation-cured glass cementitious composites.
- To marketize the proposed method, further studies should investigate carbonation curing of large scale glass concrete elements to verify the implementability of this method to filed applications.
- The process in this study works optimally for the selected type of glass, i.e. clear glass that contains around 75% SiO_2. The optimal process for other types of glass may be different. Future studies should propose standard optimized method for different types of glass concrete mixtures with various types of glass to better commercialize manufacturing of glass concrete.

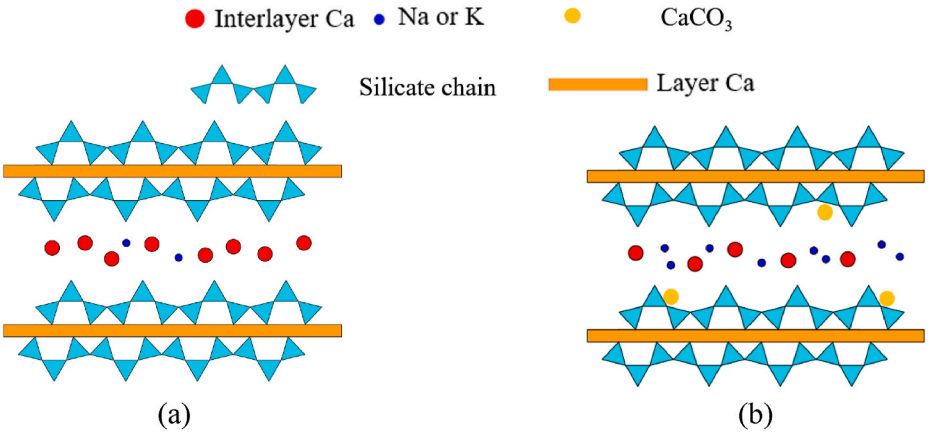

Fig. 12. Binding of alkali metals by C–S–H in: (a) Uncarbonated sample; and (b) carbonated sample.

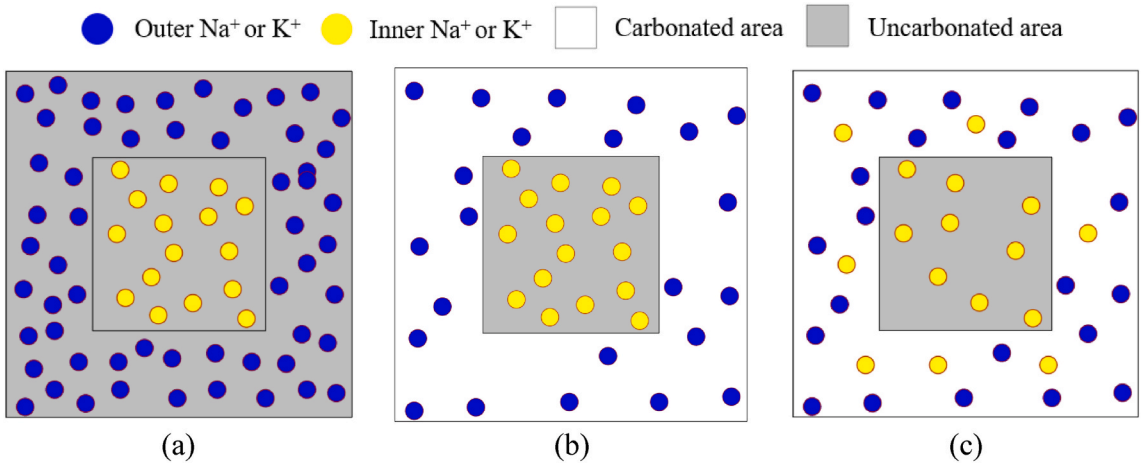

Fig. 13. Migration of alkali metal ions by carbonation: (a) Evenly-distributed alkali metals; (b) alkali metal binding in carbonated area; and (c) migration of alkali metals from midsection to the carbonated front-end.

CRediT authorship contribution statement

Zhuo Liu: Data generation, Formal analysis, Visualization, Writing – original draft. **Caijun Shi:** Conceptualization, Project administration, Supervision, Writing – review & editing. **Qiantao Shi:** Formal analysis, Writing – review & editing. **Xiao Tan:** Data generation, Writing – review & editing. **Weina Meng:** Conceptualization, Funding acquisition, Resources, Methodology, Supervision, Writing – review & editing.

Declaration of competing interest

The authors declare that they have no known competing financial interests or personal relationships that could have appeared to influence the work reported in this paper.

Data availability

Data will be made available on request.

Acknowledgement

This research was partially funded by National Science and Foundation (award number: CMMI 2046407) and the New Jersey Department of Transportation funded Task Order 388 – Bridge Resource Program 2021–2021 RIME, Contract ID Number: 21–5086.

References

Aiqin, W., Chengzhi, Z., Mingshu, T., Ningsheng, Z., 1999. ASR in mortar bars containing silica glass in combination with high alkali and high fly ash contents. Cement Concr. Compos. 21 (5–6), 375–381.
Aliabdo, A.A., Abd Elmoaty, M., Aboshama, A.Y., 2016. Utilization of waste glass powder in the production of cement and concrete. Construct. Build. Mater. 124, 866–877.
Alonso, M., Garcia, C., Walker, C., 2012. Development of an Accurate pH Measurement Methodology for the Pore Fluids of Low pH Cementitious Materials. Swedish Nuclear Fuel and Waste Management Co.
Ashraf, W., 2016. Carbonation of cement-based materials: challenges and opportunities. Construct. Build. Mater. 120, 558–570.
Ashraf, W., Olek, J., Sahu, S., 2019. Phase evolution and strength development during carbonation of low-lime calcium silicate cement (CSC). Construct. Build. Mater. 210, 473–482.
ASTM C109, 2020. Standard Test Method for Compressive Strength of Hydraulic Cement Mortars. ASTM International West Conshohocken, , PA, USA.
ASTM C136-06, Standard test method for sieve analysis of fine and coarse aggregates, 2015. ASTM International West Conshohocken, , PA, USA.
ASTM C1567, 2013. Standard Test Method for Determining the Potential Alkali-Silica Reactivity of Combinations of Cementitious Materials and Aggregate. ASTM International West Conshohocken, , PA, USA (accelerated mortar-bar method).
Belda Revert, A., De Weerdt, K., Hornbostel, K., Geiker, M.R., 2018. Carbonation-induced corrosion: investigation of the corrosion onset. Construct. Build. Mater. 162, 847–856.
Bernard, E., Yan, Y., Lothenbach, B., 2021. Effective cation exchange capacity of calcium silicate hydrates (CSH). Cement Concr. Res. 143, 106393.
Borges, P.H.R., Costa, J.O., Milestone, N.B., Lynsdale, C.J., Streatfield, R.E., 2010. Carbonation of CH and C-S-H in composite cement pastes containing high amounts of BFS. Cement Concr. Res. 40 (2), 284–292.
Bostanci, S.C., Limbachiya, M., Kew, H., 2018. Use of recycled aggregates for low carbon and cost effective concrete construction. J. Clean. Prod. 189, 176–196.
Bueno, E.T., Paris, J.M., Clavier, K.A., Spreadbury, C., Ferraro, C.C., Townsend, T.G., 2020. A review of ground waste glass as a supplementary cementitious material: a focus on alkali-silica reaction. J. Clean. Prod. 257, 120180.
Chen, T., Gao, X., 2019. Effect of carbonation curing regime on strength and microstructure of portland cement paste. J. CO2 Util. 34, 74–86.
Corinaldesi, V., Gnappi, G., Moriconi, G., Montenero, A., 2005. Reuse of ground waste glass as aggregate for mortars. Waste Manag. 25 (2), 197–201.
De Weerdt, K., Plusquellec, G., Belda Revert, A., Geiker, M.R., Lothenbach, B., 2019a. Effect of carbonation on the pore solution of mortar. Cement Concr. Res. 118, 38–56.
De Weerdt, K., Plusquellec, G., Revert, A.B., Geiker, M., Lothenbach, B., 2019b. Effect of carbonation on the pore solution of mortar. Cement Concr. Res. 118, 38–56.
Du, H., Tan, K.H., 2013. Use of waste glass as sand in mortar: Part ii–alkali–silica reaction and mitigation methods. Cement Concr. Compos. 35 (1), 118–126.
Du, J., Meng, W., Khayat, K.H., Bao, Y., Guo, P., Lyu, Z., Abu-obeidah, A., Nassif, H., Wang, H., 2021. New development of ultra-high-performance concrete (UHPC). Compos. B Eng., 109220
Ekolu, S., Thomas, M., Hooton, R., 2007. Dual effectiveness of lithium salt in controlling both delayed ettringite formation and ASR in concretes. Cement Concr. Res. 37 (6), 942–947.
Feng, X., Thomas, M., Bremner, T., Balcom, B., Folliard, K., 2005. Studies on lithium salts to mitigate ASR-induced expansion in new concrete: a critical review. Cement Concr. Res. 35 (9), 1789–1796.
Feng, X., Thomas, M., Bremner, T., Folliard, K.J., Fournier, B., 2010. New observations on the mechanism of lithium nitrate against alkali silica reaction (ASR). Cement Concr. Res. 40 (1), 94–101.
Gong, F., Zhang, D., Sicat, E., Ueda, T., 2014. Empirical estimation of pore size distribution in cement, mortar, and concrete. J. Mater. Civ. Eng. 26 (7), 04014023.
Guo, P., Meng, W., Nassif, H., Gou, H., Bao, Y., 2020. New perspectives on recycling waste glass in manufacturing concrete for sustainable civil infrastructure. Construct. Build. Mater. 257, 119579.
Han, J., Sun, W., Pan, G., Caihui, W., 2013. In: Monitoring the Evolution of Accelerated Carbonation of Hardened Cement Pastes by X-Ray Computed Tomography, vol. 25, pp. 347–354, 3.
Hong, S.-Y., Glasser, F., 1999. Alkali binding in cement pastes: Part i. The CSH phase. Cement Concr. Res. 29 (12), 1893–1903.
Ichikawa, T., Miura, M., 2007. Modified model of alkali-silica reaction. Cement Concr. Compos. 37 (9), 1291–1297.
Jang, J.G., Lee, H.K., 2016. Microstructural densification and CO_2 uptake promoted by the carbonation curing of belite-rich portland cement. Cement Concr. Res. 82, 50–57.
Jani, Y., Hogland, W., 2014. Waste glass in the production of cement and concrete–a review. J. Environ. Chem. Eng. 2 (3), 1767–1775.
Johnston, C., 1974. Waste glass as coarse aggregate for concrete. J. Test. Eval. 2 (5), 344–350.
Kawamura, M., Fuwa, H., 2003. Effects of lithium salts on ASR gel composition and expansion of mortars. Cement Concr. Res. 33 (6), 913–919.
Kou, S., Poon, C.S., 2009. Properties of self-compacting concrete prepared with recycled glass aggregate. Cement Concr. Compos. 31 (2), 107–113.
Kumar, R., Bhattacharjee, B., 2003. Porosity, pore size distribution and in situ strength of concrete. Cement Concr. Res. 33 (1), 155–164.
L'Hôpital, E., Lothenbach, B., Scrivener, K., Kulik, D.A., 2016a. Alkali uptake in calcium alumina silicate hydrate (C-A-S-H). Cement Concr. Res. 85, 122–136.

L'Hôpital, E., Lothenbach, B., Scrivener, K., Kulik, D., 2016b. Alkali uptake in calcium alumina silicate hydrate (CASH). Cement Concr. Res. 85, 122–136.
Ling, T.-C., Poon, C.-S., 2011. Properties of architectural mortar prepared with recycled glass with different particle sizes. Mater. Des. 32 (5), 2675–2684.
Liu, Z., Meng, W., 2021. Fundamental understanding of carbonation curing and durability of carbonation-cured cement-based composites: a review. J. CO2 Util. 44, 101428.
Liu, J. Du Z., Christodoulatos, C., Conway, M., Bao, Y., Meng, W., 2022. Utilization of off-specification fly ash in preparing ultra-high-performance concrete (UHPC): mixture design, characterization, and life-cycle assessment. Resour. Conserv. Recycl. 180, 106136.
Meng, W., Khayat, K.H., 2018. Effect of graphite nanoplatelets and carbon nanofibers on rheology, hydration, shrinkage, mechanical properties, and microstructure of UHPC. Cement Concr. Res. 105, 64–71.
Mo, L., Zhang, F., Deng, M., 2016. Mechanical performance and microstructure of the calcium carbonate binders produced by carbonating steel slag paste under CO_2 curing. Cement Concr. Res. 88, 217–226.
Pan, X., Shi, C., Hu, X., Ou, Z., 2017. Effects of CO_2 surface treatment on strength and permeability of one-day-aged cement mortar. Construct. Build. Mater. 154, 1087–1095.
Pan, X., Shi, C., Farzadnia, N., Hu, X., Zheng, J., 2019. Properties and microstructure of CO_2 surface treated cement mortars with subsequent lime-saturated water curing. Cement Concr. Compos. 99, 89–99.
Park, S.B., Lee, B.C., Kim, J.H., 2004. Studies on mechanical properties of concrete containing waste glass aggregate. Cement Concr. Res. 34 (12), 2181–2189.
Plusquellec, G., Geiker, M.R., Lindgård, J., Duchesne, J., Fournier, B., De Weerdt, K., 2017. Determination of the pH and the free alkali metal content in the pore solution of concrete: review and experimental comparison. Cement Concr. Res. 96, 13–26.
Räsänen, V., Penttala, V., 2004. The pH measurement of concrete and smoothing mortar using a concrete powder suspension. Cement Concr. Res. 34 (5), 813–820.
Rostami, V., Shao, Y., Boyd, A.J., He, Z., 2012. Microstructure of cement paste subject to early carbonation curing. Cement Concr. Res. 42 (1), 186–193.
Saccani, A., Bignozzi, M.C., 2010. ASR expansion behavior of recycled glass fine aggregates in concrete. Cement Concr. Res. 40 (4), 531–536.
Sanchez, L.F.M., Fournier, B., Jolin, M., Mitchell, D., Bastien, J., 2017. Overall assessment of alkali-aggregate reaction (AAR) in concretes presenting different strengths and incorporating a wide range of reactive aggregate types and natures. Cement Concr. Res. 93, 17–31.
Šavija, B., Luković, M., 2016. Carbonation of cement paste: understanding, challenges, and opportunities. Construct. Build. Mater. 117, 285–301.
Serpa, D., Silva, A.S., De Brito, J., Pontes, J., Soares, D., 2013. ASR of mortars containing glass. Construct. Build. Mater. 47, 489–495.
Shafaatian, S.M., Akhavan, A., Maraghechi, H., Rajabipour, F.J.C., 2013. How does fly ash mitigate alkali–silica reaction (ASR) in accelerated mortar bar test (ASTM C1567)? Cement Concr. Compos. 37, 143–153.
Shao, Y., Lefort, T., Moras, S., Rodriguez, D., 2000. Studies on concrete containing ground waste glass. Cement Concr. Res. 30 (1), 91–100.
Shi, X., Tan, T.-H., Tan, K.-H., Guo, Z., 2004. Influence of concrete cover on fire resistance of reinforced concrete flexural members. J. Struct. Eng. 130 (8), 1225–1232.
Shi, C., He, F., Wu, Y., 2012. Effect of pre-conditioning on CO_2 curing of lightweight concrete blocks mixtures. Construct. Build. Mater. 26 (1), 257–267.
Shoji, M., Higuchi, T., Morioka, M., Yokozeki, K., 2015. Inhibitory effect of alkali-silica reaction by the carbonation reaction. Cement Science and Concrete Technology 69 (1), 504–510.
Song, W., Yi, J., Wu, H., He, X., Song, Q., Yin, J., 2019. Effect of carbon fiber on mechanical properties and dimensional stability of concrete incorporated with granulated-blast furnace slag. J. Clean. Prod. 238, 117819.
Sun, B., Wu, H., Song, W., Li, Z., Yu, J., 2019. Design methodology and mechanical properties of superabsorbent polymer (SAP) cement-based materials. Construct. Build. Mater. 204, 440–449.
Taha, B., Nounu, G., 2008. Properties of concrete contains mixed colour waste recycled glass as sand and cement replacement. Construct. Build. Mater. 22 (5), 713–720.
Tapas, M.J., Sofia, L., Vessalas, K., Thomas, P., Sirivivatnanon, V., Scrivener, K., 2021. Efficacy of scms to mitigate ASR in systems with higher alkali contents assessed by pore solution method. Cement Concr. Res. 142, 106353.
Thomas, M., 2011. The effect of supplementary cementing materials on alkali-silica reaction: a review. Cement Concr. Res. 41 (12), 1224–1231.
Topcu, I.B., Canbaz, M., 2004. Properties of concrete containing waste glass. Cement Concr. Res. 34 (2), 267–274.
U. EPA, 2020. Advancing Sustainable Materials Management: Facts and Figures Report. US EPA, Washington, DC, USA.
Yang, S., Poon, C.S., Ling, T.C., 2019. Distribution of ASR gel in conventional wet-mix glass mortars and mechanically produced dry-mix glass blocks. Construct. Build. Mater. 229, 116916.
Zhan, B., Poon, C., Shi, C., 2013. CO_2 curing for improving the properties of concrete blocks containing recycled aggregates. Cement Concr. Compos. 42, 1–8.
Zhan, B.J., Xuan, D.X., Poon, C.S., Shi, C.J., 2019. Mechanism for rapid hardening of cement pastes under coupled CO_2-water curing regime. Cement Concr. Compos. 97, 78–88.
Zhan, B.J., Xuan, D.X., Poon, C.S., Scrivener, K.L., 2021. Multi-scale investigation on mechanical behavior and microstructural alteration of CSH in carbonated alite paste. Cement Concr. Res. 144, 106448.
Zhang, D., Shao, Y., 2016. Early age carbonation curing for precast reinforced concretes. Construct. Build. Mater. 113, 134–143.
Zhang, D., Shao, Y., 2018. Surface scaling of CO_2-cured concrete exposed to freeze-thaw cycles. J. CO2 Util. 27, 137–144.
Zhang, D., Li, V.C., Ellis, B.R., 2018. Optimal pre-hydration age for CO_2 sequestration through portland cement carbonation. ACS Sustain. Chem. Eng. 6 (12), 15976–15981.
Zhang, D., Liu, T., Shao, Y., 2020. Weathering carbonation behavior of concrete subject to early-age carbonation curing. J. Mater. Civ. Eng. 32 (4), 04020038.
Zheng, K., 2016. Pozzolanic reaction of glass powder and its role in controlling alkali–silica reaction. Cement Concr. Compos. 67, 30–38.